HHS Public Access

Author manuscript

ACS Nano. Author manuscript; available in PMC 2018 March 22.

Published in final edited form as:

ACS Nano. 2016 October 25; 10(10): 9536–9542. doi:10.1021/acsnano.6b04795.

An Enteric Micromotor Can Selectively Position and Spontaneously Propel in the Gastrointestinal Tract

Jinxing Li[†], **Soracha Thamphiwatana**[†], **Wenjuan Liu**[†], **Berta Esteban-Fernández de Ávila**, **Pavimol Angsantikul**, **Elodie Sandraz**, **Jianxing Wang**, **Tailin Xu**, **Fernando Soto**, **Valentin Ramez**, **Xiaolei Wang**, **Weiwei Gao**, **Liangfang Zhang**[*], and **Joseph Wang**[*]

Department of Nanoengineering, University of California San Diego, La Jolla, CA 92093, USA

Abstract

The gastrointestinal (GI) tract, which hosts hundreds of bacteria species, becomes the most exciting organ for the emerging microbiome research. Some of these GI microbes are hostile and cause a variety of diseases. These bacteria colonize in different segments of the GI tract dependent on the local physicochemical and biological factors. Therefore, selectively locating therapeutic or imaging agents to specific GI segments is of significant importance for studying gut microbiome and treating various GI-related diseases. Herein, we demonstrate an enteric micromotor system capable of precise positioning and controllable retention in desired segments of the GI tract. These motors, consisting of magnesium-based tubular micromotors coated with an enteric polymer layer, act as a robust nanobiotechnology tool for site-specific GI delivery. The micromotors can deliver payload to particular location *via* dissolution of their enteric coating to activate their propulsion at the target site towards localized tissue penetration and retention.

TOC image

[*]**Corresponding authors:** josephwang@ucsd.edu and zhang@ucsd.edu.
[†]These authors contributed equally to this work.

Supporting information. The Supporting Information is available free of charge via the Internet at http://pubs.acs.org.

Author Contributions

All authors have given approval to the final version of the manuscript.

Notes. The authors declare no competing financial interest.

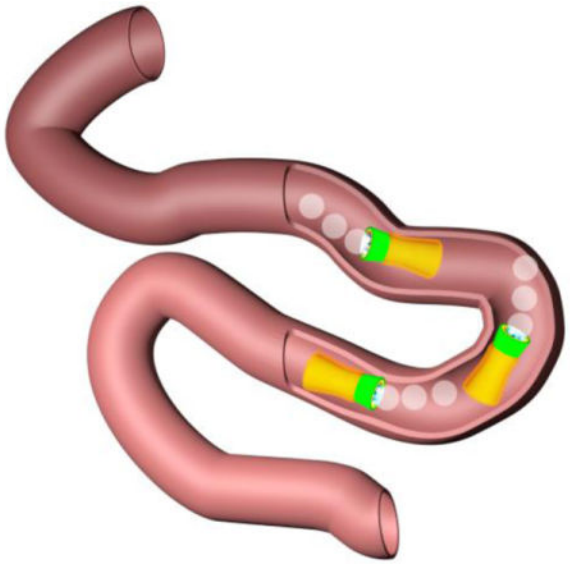

Keywords

Micromotor; gastrointestinal tract; active delivery; pH-responsive polymer; biodistribution

Microbiomes play important roles in the health of many animals, including human beings, thus have attracted intense research interest.[1,2] While most of the GI microbes live in harmony with the host, some are hostile and cause a variety of diseases. These bacteria colonize in different segments of the GI tract, dependent on local factors.[3,4] Therefore, selectively locating therapeutic or imaging agents to specific segments of the GI tract is of considerable interest.[5] Ideal GI delivery system should protect the cargos en-route and accurately locate them to the site of action. Upon arrival at destination, the carrier should retain there for unloading the cargos. Fulfilling this goal is hampered by the body's natural physiological and structural barriers. As a result, it still remains an unmet need to develop a biocompatible nano/micro-scale device that can selectively position in a specific segment of the GI tract and actively penetrate into the tissue for prolonged retention.

Over the past decade, remarkable advances have been made in the development of artificial micromotors, which are tiny devices that convert locally supplied fuels or externally provided energy to propelling force and movement.[6–14] These micromotors have proved useful for performing diverse biomedical tasks, including transport of cargos, biosensing and imaging, and target isolation.[15–18] After nearly ten years of basic research on the synthesis and characterization of artificial micromotors in test-tubes, the field has recently reached a new milestone where the performance and functionality of the motors were being evaluated in live bodies. For instance, the *in vivo* evaluation of synthetic micromotors demonstrated that acid-powered motors can function in a live mouse's stomach for gastric cargo delivery without causing toxic effects.[19] Magnetic actuation and navigation were also applied to control the swarming of artificial bacterial flagella *in vivo*.[20] These studies demonstrate that motor-based active delivery approaches offer attractive features for localized cargo delivery.

In this study, we developed an enteric micromotor consisting of a magnesium (Mg)-based motor body with an enteric polymer coating. The Mg body allows for spontaneous propulsion in intestinal fluid while the coating, which is stable in acidic conditions but soluble in neutral or alkaline media,[21,22] enables accurate positioning in the GI tract. The enteric coating can shield the motors from acidic gastric fluid environment (pH 1~3), but dissolves in intestinal fluid (pH 6~7) to expose the motors to their fuel and start the movement. By tailoring the thickness of the enteric coating, we can tune the time required to dissolve the polymer layer, thereby controlling the distance that the motors can travel in the GI tract before their propulsion is activated. Upon activation the motors will propel and penetrate into the local tissue and retain there to release payloads. The properties and functions of the synthesized enteric magnesium micromotors (EMgMs) are evaluated in a mouse model. The *in vivo* results demonstrate that these motors can safely pass through the gastric fluid and accurately activate in the GI tract without causing noticeable acute toxicity.

RESULTS AND DISCUSSION

Figure 1a and Supporting Video 1 illustrate the operation principle of the EMgMs that can selectively position and spontaneously propel in the GI tract by using the pH-sensitive coating which dissolves in intestinal fluid (pH 6~7). Figure 1b shows the fabrication processes of EMgMs, where a template-electrodeposition method is combined with a particle-infiltration technique by packing Mg microparticles within template-synthesized PEDOT/Au microtubes with uniform diameter of 5 μm (Supporting Video 2). The template-synthesized PEDOT/Au microtubes serve as robust microcontainers for Mg microparticles loading while the Au is used as a trace element and a model cargo for *in vivo* biodistribution study. Note that Mg is a biocompatible trace element vital for many bodily functions and that the reaction of Mg microparticles with water is used to generate propulsion.[23,24]

Figure 1c and Supporting Figure 1 display the top and side views, respectively, of Mg particles infiltrated into a PEDOT/Au microtube. These SEM images and EDX mapping confirm that the microtube can be successfully loaded with Mg particles, while the interparticle space could be potentially filled with therapeutic or imaging payloads. The motors are subsequently coated with methacrylate-based polymer Eudragit L100-55, which has been used for protecting oral drug capsules from the acidic gastric fluid.[21,22,25] The SEM image and EDX mapping in Figure 1d show the side view of a micromotor with a smooth enteric polymer coverage. Upon fabrication of the EMgMs, we first evaluated their propulsion performance in intestinal fluid. The microscopy images of Figure 1e (corresponding to Supporting Videos 3), demonstrate effective movement of a single and multiple EMgMs in intestinal fluid simulant. Hydrogen bubbles propel the motors for approximately 1 min with average speed of 60 μm/s, demonstrating water-powered microtubular motors that can efficiently propel and function in intestinal fluid.

To evaluate the feasibility of precisely tuning the activation time of EMgMs after entering the GI tract, the micromotors - with an original diameter of 5 μm – were modified with enteric polymer coatings of three different thicknesses (0.3, 0.8 and 1.2 μm) and were tested in gastric and intestine fluids. The thickness of the polymeric coating was adjusted by using three enteric polymer concentrations of 6.5%, 10.0% and 12.5 % (w/v), which resulted in

average EMgMs diameters of 5.6, 6.6 and 7.4 μm, respectively. Figure 2a shows that EMgMs with thin coating display no bubble generation upon immersing in gastric acid for over 150 minutes, reflecting the shielding ability of the polymer in strongly acidic gastric environment. Upon changing to intestinal fluid, these EMgMs display a burst of bubble generation and efficient propulsion within 20 minutes (Figure 2b). The efficient propulsion eventually leads to a dynamic distribution of the micromotors to different locations. Medium and thick enteric coatings are able to delay the bubble generation and micromotor propulsion to 60 minutes and 150 minutes after immersion in intestinal fluid, respectively (Figure 2c and d). Supporting Video 4 shows the delayed actuation of EMgMs in the intestinal fluid.

Figure 2e shows the quantitative results of the release and activation of EMgMs with different enteric coatings in intestinal fluid. Based upon the statistical analysis of about 400 motors for each group, thin polymer coating results in over 75% of EMgMs activated in intestinal fluid within 10 min, indicating that the propulsion occurs in the upper segment of the GI tract. In contrast, for a medium-thickness coating, a very slow activation is observed between 30 and 45 minutes, followed by a rapid activation of about 75% of EMgMs between 50 to 70 minutes, indicating the motors localize at the middle segment of the GI tract. EMgMs coated by a thick polymer layer display very slow activation up to 2 hours, followed by rapid activation of 80% EMgMs at 3 hours, indicating that these motors can reach the lower segment of the GI tract. These results verify the possibility of selectively position the motors in different regions of the GI tract by controlling the coating thickness.

The ability of EMgMs to selectively localize at desirable segments of the GI tract was evaluated *in vivo* using a mouse model. In the study, four groups (n=3) of mice were assigned to receive EMgMs with three different polymer thicknesses and uncoated micromotors, respectively. Upon oral administration of the motors for 6 hours, the mice were euthanized, and their stomach and entire GI tract were collected to evaluate the biodistribution and retention of the motors. Specifically, the mouse GI tract was sliced into three segments corresponding to duodenum, jejunum and ileum of the GI tract (Figure 3a) for separate inspection. Figure 3b displays the distribution of the micromotors in these three GI segments and the stomach for the four tested groups. The uncoated micromotors display significant (79%) retention in the stomach, reflecting their efficient activation and propulsion in the stomach (Figure 3b i). The enteric polymer coatings offer robust protection of the micromotors in the stomach and thus enhance their delivery efficiency to the GI tract. A small fraction (16%) of EMgMs with thin enteric coating retained in the stomach (Figure 3b ii) while minimal micromotors were detected in the stomach for EMgMs with medium and thick coatings (Figure 3b iii and iv). In contrast, Figure 3b ii–iv illustrate that 75%, 67% and 54% of the motors retained in the duodenum, jejunum and ileum for EMgMs with thin, medium and thick enteric coatings, respectively. These results demonstrate that controlling the coating thickness, and hence the exposure and activation times of the motors, has a profound effect upon the biodistribution of EMgMs within the GI tract.

We further studied the retention of the EMgMs with medium coating in mouse GI tract by orally administrating fluorescently labeled EMgMs (See characterization in Supporting Figure 2). At 6 and 12 hours after EMgMs administration, the entire GI tract was excised for fluorescence imaging, as shown in Fig 3c and Supporting Figure 3. The image obtained from

GI tract collected at 6 hours showed the strongest fluorescence in jejunum and the signal remained at the site at 12 hours, which was about four-fold longer than typical gastric emptying times in mouse GI tract.[26] In contrast, when mice were treated with phosphate-buffered saline (PBS) control, there was no detectable fluorescence signal in the GI tissue; some signal observed in the stomach is attributed to the food self-fluorescence. The luminal surfaces of the intestines are covered by a mucus layer, consisting of large and highly glycosylated proteins, which serve as the front line of protection of GI tract.[27] When the cylindrical Mg-loaded motors are locally released and activated in the GI tract, they will propel and collide with the porous, slimy mucus layer and can be readily trapped within the gel-like mucus, leading to an enhanced local retention. To test our hypothesis that the active propulsion of the motors is critical for enhanced local retention, we compared the retention of EMgMs with medium polymer coating with that of inert silica-microsphere loaded PEDOT/Au microtubes (with the same polymer coating). As shown in Supporting Figure 4. The latter are inert in the intestinal environment fluid and do not exhibit autonomous propulsion when released. These control micomotors displayed a significantly lower fluorescence intensity, compared to the EMgMs, reflecting their greatly reduced retention in the jejunum under the same experimental conditions and coatings (Supporting Figure 5). Such observations are similar to our early work which demonstrated that the propulsion of Zn-based micromotors in the acidic stomach environment greatly improved their tissue penetration and retention.[19] In the present work, we obtained similar results with highly enhanced retention (up to 24 hrs) associated with propulsive micromotors. Overall, self-propelled micromotors lead to a dramatically improved localized retention of their payloads in the intestine compared to the passive diffusion and dispersion of inert payloads. These data verify that both the enteric polymer coating and the propulsion of the Mg-based micromotors are critical for their accurate position and enhanced retention simultaneously in desired segment of the GI tract.

Finally, the toxicity profile of the EMgMs in the GI tract was investigated. Mice were orally administrated with PBS buffer (Figure 4a–c) or suspension of EMgMs with medium polymer coating thickness (Figure 4d–f) and monitored for general toxicity signs every 2 hours for the first 10 hours post administration. No physiological symptoms such as lethargy, rough fur, or diarrhea were observed in both groups. Then, the GI tract was dissected and sectioned for histological evaluation 24 hours after administration. The tissues were first stained with hematoxylin and eosin (H&E) (Figure 4 a, b, d, e). We did not observe apparent alteration of gastric and intestinal mucosal epithelial architectures or differences in the crypt and villus length and number, or mucosal thickness, between the PBS and motors-treated groups. There was also no infiltration of immune cells such as neutrophils, lymphocytes, or macrophages into the mucosa and submucosa, indicating no sign of tissue inflammation. Furthermore, the deparaffinized mouse gastric tissue sections of motor-treated mice showed no difference in apoptotic gastric and intestinal epithelial compared to the PBS control, as indicated by positive staining cells in TUNEL assay (Figure 4 c, f).[28,29] Overall, the *in vivo* toxicity studies demonstrate no apparent GI mucosal epithelial morphology change or inflammation, suggesting that the EMgMs are biocompatible and safe for oral administration in mouse model.

CONCLUSIONS

A desirable GI delivery system should be able to protect the cargos en-route and accurately locate them to the site of action. Upon arrival at destination, the carrier should retain at the site for complete unloading of the cargos. The reported enteric magnesium micromotors provide an exciting thrust towards achieving such goal. By simply tuning the thickness of the pH-sensitive polymer coating it is feasible to selectively activate the propulsion of the water-powered micromotors, and thus to control their tissue penetration and retention at desired regions of the GI tract. Such combination of accurate positioning and active propulsion demonstrate that a microscale robot can achieve desired biodistribution and enhanced retention simultaneously in the GI tract; it is therefore of particular importance for the emerging microbiome research. Furthermore, the use of advanced pH-sensitive materials for precise local manipulation of microrobot for site-specific active delivery (compared to conventional passive-diffusion-driven delivery vehicles) is expected to pioneer novel delivery approaches and advance the emerging field of medical nano/micromotors and nanorobotics. While future studies are warranted to validate the delivery efficiency and therapeutic efficacy, the micromotor-based GI transporter system offers innovative combination of accurate positioning and active propulsion towards effective localized GI delivery of cargos and personalized treatment of GI diseases and disorders.

Methods

Synthesis of EMgMs

Polycarbonate (PC) membrane templates (110607, Whatman, NJ, USA) with pore sizes of 5 μm were used for fabricating the Mg-based micromotors. A 75 nm gold film was sputtered on one side of the porous membrane to serve as a working electrode using the Denton Discovery 18 (Moorestown, NJ, USA). A Pt wire and an Ag/AgCl (with 1 M KCl) were used as counter and reference electrodes, respectively. The membrane was then assembled in a plating cell with aluminum foil serving as a contact. All electrochemical deposition steps were carried out at room temperature (22 °C). First, the outer PEDOT layer of the microtubes was prepared by electropolymerization at +0.80 V using a charge of 0.2 C from a plating solution containing 15 mM EDOT, 7.5 mM KNO_3, and 100 mM sodium dodecyl sulfate (SDS); subsequently, a gold layer was deposited at −0.9 V from a commercial gold plating solution (Orotemp 24 RTU RACK; Technic Inc., USA) with a total charge of 0.6 C. After electrochemical deposition, the sputtered gold layer was completely removed by mechanical polishing with 3 μm alumina slurry. In order to get the Mg microparticles with favorable size to be loaded in the prepared PEDOT/Au microtube with a diameter of ~5 μm, the microparticles were collected from the commercial ones (size 0.2–50 μm catalog #FMW20, TangShanWeiHao Magnesium Powder Co., China). Vacuum infiltration process by a 5 μm Polycarbonate membrane (110607, Whatman, NJ, USA) was used to remove the Mg microparticles with size larger than 5 μm, then another vacuum infiltration process using a 1 μm Polycarbonate membrane (110607, Whatman, NJ, USA) was used to remove the Mg microparticles with size smaller than 1 μm. The obtained Mg microparticles with size of 1–5 μm were then dispersed in isopropanol with a concentration of 10 mg/mL. Thereafter, the Mg microparticle suspension was pumped into the polished polycarbonate templates with

electrodeposited PEDOT/Au microtubes using vacuum infiltration. A polycarbonate membrane with a pore size of 15 nm was placed below the 5 μm diameter PC membrane to retain the magnesium microparticles within the upper PEDOT/Au microtubes. The vacuum infiltration process was performed for 2 hours to ensure full loading of Mg microparticles in the microtubes. The polycarbonate membrane was then dissolved in methylene chloride for 2 h to completely release the micromotors, *e.g.* the Mg microparticles loaded PEDOT/Au microtubes. The micromotors were then collected by a sediment process and washed with methylene chloride and isopropanol (3 times each one). Fluorescent Mg-based micromotors were prepared by using the Mg microparticle suspension dissolved with a Rhodamine 6G dye (83697, SIGMA, USA) with a concentration of 2 μg/mL.

A commercial enteric polymer (Eudragit L100-55; Evonik Industries, Germany) was chosen to be coated on the Mg-based micromotors to prevent the Mg microparticles from reacting in stomach fluid thus ensuring their safe reaching to the GI tract. First, a batch of Mg-based micromotors (dissolved from one whole piece of PC membrane) was collected in 0.1 mL isopropanol solution. Then Eudragit L 100-55 was dissolved into isopropanol solution with three different concentrations of 6.5%, 10.0% and 12.5 % (w/v) to prepare the EMgMs with different coating thicknesses. The micromotor suspension was then mixed with Eudragit L100-55 solution with the above three different concentrations, and then dispersed in to a paraffin matrix for a solvent evaporation process. The obtained structures were then solidified with hexanes and a following freeze drying process. Finally, a soft annealing of 130 °C for 10 min to ensure the complete sealing of the Mg-based micromotors. The original diameter of the micromotors without polymer coating is 5 μm, as defined by the micropores of the polycarbonate membrane template. The enteric coating thicknesses were examined by SEM. For the three enteric polymer concentration of 6.5%, 10.0% and 12.5 % (w/v), a coating thickness of 0.3, 0.8 and 1.2 μm was calculated by polymer-coated micromotors with an average diameters of 5.6, 6.8 and 7.4 μm, respectively.

To make the silica microspheres-loaded control micromotors, a suspension of silica microspheres (diameter 1.21 μm, Bangs Lot# 8348, Fisher, IN, USA) were added into the PEDOT/Au microtubes, instead of Mg microparticles. An enteric polymer coating, with a thickness of 0.8 μm, was then coated on these silica-microspheres loaded micromotors by same method described above using a polymer concentration of 10.0%. The resulting coated silica-microspheres loaded micromotors were then used as control micromotors without movement in the intestinal fluid.

In vitro release study

In vitro release of the EMgMs was performed using gastric fluid simulant and intestinal fluid simulant, respectively. Videos of micromotor propulsion were captured by an inverted optical microscope (Nikon Instrument Inc. Ti-S/L100), coupled with a 40× microscope objective, a Hamamatsu digital camera C11440 using the NIS-Elements AR 3.2 software. In each test of the release study, EMgMs were dispersed on a glass slide with PDMS cell to prevent the evaporation of the liquid during the observation. Normally about 400 micromotors were in the view under the 4× microscope objective. The CCD camera is set to take a microscopy image every minute, while the micromotor which is generating bubble or

moved from its original place in the imaging is consider as being released. The time-dependent release rate is calculated in each test then averaged as the statistical results (n=6).

In vivo GI tract site-specific localization and retention studies

For *in vivo* GI tract site-specific localization study, 8 weeks old ICR male mice were purchased from Harlan Laboratory (Indianapolis, IN). Mice were gavaged with 0.3 mL of suspension of uncoated Mg-based micromotors or EMgMs with thin, medium, or thick enteric coatings (n=6). GI tracts including stomach, duodenum, jejunum, and ileum from each mouse were collected at 6 hours after administration. The tissues were rinsed with PBS. Each section was placed in a glass vial and 3 mL of aqua regia consisting of concentrated nitric acid and hydrochloric acid (Sigma-Aldrich, St. Louis, MO, USA) in the ratio of 1:3 was added into the tissue for 12 hours at room temperature; this was followed by annealing at 80 °C for 6 hours in order to remove the acids and then resuspended with 5 mL DI water. Analysis of the amount of micromotors retained in each part of GI tract was carried out by measuring their embedded Au content using inductively coupled plasma-mass spectrometry (ICP-MS). For *in vivo* retention study, mice (n=6) were fed with alfalfa-free food from LabDiet (St. Louis, MO, USA) for 2 weeks prior to the experiment. A 0.3 mL suspension of fluorescence-labeled EMgMs with medium thickness of enteric coating was administered orally. At 6 and 12 hours after administration, the GI tracts were dissected, rinsed with PBS, and then imaged using an intelligent visual inspection system (IVIS). A 0.3 mL PBS was given to control mice and tissues were collected and imaged at 6 hours after administration. For *in vivo* retention study comparing the propulsive EMgMs with inert silica microspheres loaded micromotors, one group of the mice were orally administrated with a 0.3 mL suspension of fluorescence-labeled EMgMs with medium thickness of enteric coating, while another group were orally administrated with a 0.3 mL suspension of silica-microsphere loaded PEDOT/Au microtubes coated with medium thickness of enteric coating. At 6 hours after administration, the GI tracts were dissected, rinsed with PBS, and then imaged using an intelligent visual inspection system (IVIS).

In vivo toxicity study

To investigate the acute toxicity of EMgMs, 8 weeks old ICR male mice were oral-gavaged with 0.3 mL suspension of EMgMs with medium thickness of enteric coating. Healthy mice treated with PBS were used as a negative control. Mice were sacrificed at 24 hours after the administration. The stomach and small intestine were collected. The stomach was cut open along the greater curvature, and the gastric content was removed. The small intestine was cut to small sections as duodenum, jejunum, and ileum, and rinsed inside with PBS to remove internal residues. The tissues were put in tissue cassettes and fixed with 10% buffered formalin for 15 hours, then moved into 70% ethanol, and then embedded in paraffin. The tissue sections were cut with 5 μm thickness and stained with hematoxylin and eosin (H&E) assay. The apoptosis cells were evaluated by terminal deoxynucleotidyl transferase-mediated dUTP nick-end labeling (TUNEL) assay using ApopTag® from EMD Millipore (Billerica, MA, USA). The stained sections were visualized by the Hamamatsu NanoZoomer 2.0HT.

Supplementary Material

Refer to Web version on PubMed Central for supplementary material.

Acknowledgments

This work is supported by the Defense Threat Reduction Agency Joint Science and Technology Office for Chemical and Biological Defense (Grant Numbers HDTRA1-13-1-0002 and HDTRA1-14-1-0064) and by the National Institute of Diabetes and Digestive and Kidney Diseases of the National Institutes of Health (Award Number R01DK095168).

References

1. Huttenhower C, Gevers D, Knight R, Abubucker S, Badger JH, Chinwalla AT, Creasy HH, Earl AM, FitzGerald MG, Fulton RS, Giglio MG, Hallsworth-Pepin K, Lobos EA, Madupu R, Magrini V, Martin JC, Mitreva M, Muzny DM, Sodergren EJ, Versalovic J, et al. Human Microbiome Project Consortium Consortium. Structure, Function and Diversity of the Healthy Human Microbiome. Nature. 2012; 486:207–214. [PubMed: 22699609]
2. Biteen JS, Blainey PC, Cardon ZC, Chun M, Church JM, Dorrestein PC, Fraser SE, Gilbert JA, Jansson JK, Knight R, Miller JF, Ozcan A, Prather KA, Quake SR, Ruby EG, Silver PA, Taha S, Engh G, Weiss PS, Wong GCL, et al. Tools for the Microbiome: Nano and Beyond. ACS Nano. 2016; 10:6–37. [PubMed: 26695070]
3. Kamada N, Seo S-U, Chen GY, Núñez G. Role of the Gut Microbiota in Immunity and Inflammatory Disease. Nat Rev Immunol. 2013; 13:321–335. [PubMed: 23618829]
4. Goodrich JK, Di Rienzi SC, Poole AC, Koren O, Walters WA, Caporaso JG, Knight R, Ley RE. Conducting a Microbiome Study. Cell. 2014; 158:250–262. [PubMed: 25036628]
5. Traverso G, Langer R. Perspective: Special Delivery for the Gut. Nature. 2015; 519:S19. [PubMed: 25806494]
6. Wang, J. Nanomachines: Fundamentals and Applications. Wiley-VCH; Weinheim, Germany: 2013.
7. Wilson DA, Nolte RJ, van Hest JC. Autonomous Movement of Platinum-loaded Stomatocytes. Nat Chem. 2012; 4:268–274. [PubMed: 22437710]
8. Mallouk TE, Sen A. Powering Nanorobots. Sci Am. 2009; 300:72–77.
9. Loget G, Kuhn A. Electric Field-induced Chemical Locomotion of Conducting Objects. Nat Commun. 2011; 2:535. [PubMed: 22086336]
10. Sánchez S, Soler L, Katuri J. Chemically Powered Micro- and Nanomotors. Angew Chem Int Ed. 2015; 54:1414–1444.
11. Wang H, Pumera M. Fabrication of Micro/nanoscale Motors. Chem Rev. 2015; 115:8704–8735. [PubMed: 26234432]
12. Palagi S, Mark AG, Reigh SY, Melde K, Qiu T, Zeng H, Parmeggiani C, Martella D, Sanchez-Castillo A, Kapernaum N, Giesselmann F, Wiersma DS, Lauga E, Fischer P. Structured Light Enables Biomimetic Swimming and Versatile Locomotion of Photoresponsive Soft Microrobots. Nat Mater. 2016; 15:647–653. [PubMed: 26878315]
13. Li J, Rozen I, Wang J. Rocket Science at the Nanoscale. ACS Nano. 2016; 10:5619–5634. [PubMed: 27219742]
14. Lin X, Wu Z, Wu Y, Xuan M, He Q. Self-propelled Micro-/nanomotors Based on Controlled Assembled Architectures. Adv Mater. 2015; 28:1060–1072. [PubMed: 26421653]
15. Wang J, Gao W. Nano/microscale Motors: Biomedical Opportunities and Challenges. ACS Nano. 2012; 6:5745–5751. [PubMed: 22770233]
16. Peyer KE, Zhang L, Nelson BJ. Bio-inspired Magnetic Swimming Microrobots for Biomedical Applications. Nanoscale. 2013; 5:1259–1272. [PubMed: 23165991]
17. Baylis JR, Yeon JH, Thomson MH, Kazerooni A, Wang X, St John AE, Lim EB, Chien D, Lee A, Zhang JQ, Piret JM, Machan LS, Burke TF, White NJ, Kastrup CJ. Self–propelled Particles that Transport Cargo Through Flowing Blood and Halt Hemorrhage. Sci Adv. 2015; 1:e1500379. [PubMed: 26601282]

18. Esteban-Fernández de ´vila B, Martin A, Soto F, Lopez-Ramirez MA, Campuzano S, Vasquez-Machado GM, Gao W, Zhang L, Wang J. Single Cell Real-time miRNAs Sensing Based on Nanomotors. ACS Nano. 2015; 9:6756–6764. [PubMed: 26035455]
19. Gao W, Dong D, Thamphiwatana S, Li J, Gao W, Zhang L, Wang J. Artificial Micromotors in the Mouse's Stomach: A Step Toward *In vivo* Use of Synthetic Motors. ACS Nano. 2015; 9:117–123. [PubMed: 25549040]
20. Servant A, Qiu F, Mazza M, Kostarelos K, Nelson B. J. Controlled *In vivo* Swimming of a Swarm of Bacteria-like Microrobotic Flagella. Adv Mater. 2015; 27:2981–2988. [PubMed: 25850420]
21. Zhang S, Bellinger AM, Glettig DL, Barman R, Lucy Lee Y-A, Zhu J, Cleveland C, Montgomery VA, Gu L, Nash LD, Maitland DJ, Langer R, Traverso G. A pH-responsive Supramolecular Polymer Gel as an Enteric Elastomer for Use in Gastric Devices. Nat Mater. 2015; 14:1065–1071. [PubMed: 26213897]
22. Zhu Q, Talton J, Zhang G, Cunningham T, Wang Z, Waters RC, Kirk J, Eppler B, Klinman DM, Sui Y, Gagnon S, Belyakov IM, Mumper RJ, Berzofsky JA. Large Intestine-targeted, Nanoparticle-releasing Oral Vaccine to Control Genitorectal Viral Infection. Nat Med. 2012; 18:1291–1296. [PubMed: 22797811]
23. Jones DDG, Masterson H. Effect of Chloride Concentration on the Aqueous Corrosion of a Magnesium Alloy. Nature. 1961; 191:165–166.
24. Gao W, Feng X, Pei A, Gu Y, Li J, Wang J. Seawater-driven Magnesium Based Janus Micromotors for Environmental Remediation. Nanoscale. 2013; 5:4696–4700. [PubMed: 23640547]
25. Lautenschläger C, Schmidt C, Fischer D, Stallmach A. Drug Delivery Strategies in the Therapy of Inflammatory Bowel Disease. Adv Drug Deliv Rev. 2014; 71:58–76. [PubMed: 24157534]
26. Bennink RJ, De Jonge WJ, Symonds EL, van den Wijngaard RM, Spijkerboer AL, Benninga MA, Boeckxstaens GE. Validation of Gastric-emptying Scintigraphy of Solids and Liquids in Mice Using Dedicated Animal Pinhole Scintigraphy. J Nucl Med. 2003; 44:1099–1104. [PubMed: 12843228]
27. Johansson Malin EV, Sjövall H, Hansson GC. The gastrointestinal mucus system in health and disease. Nat Rev Gastroenterol Hepatol. 2013; 10:352–361. [PubMed: 23478383]
28. Thamphiwatana S, Gao W, Obonyo M, Zhang L. *In vivo* Treatment of Helicobacter Pylori Infection with Liposomal Linolenic Acid Reduces Colonization and Ameliorates Inflammation. Proc Natl Acad Sci. 2014; 111:17600–17605. [PubMed: 25422427]
29. Banerjee A, Thamphiwatana S, Carmona EM, Rickman B, Doran KS, Obonyo M. Deficiency of the Myeloid Differentiation Primary Response Molecule MyD88 Leads to an Early and Rapid Development of Helicobacter-induced Gastric Malignancy. Infect Immun. 2014; 82:356–363. [PubMed: 24166959]

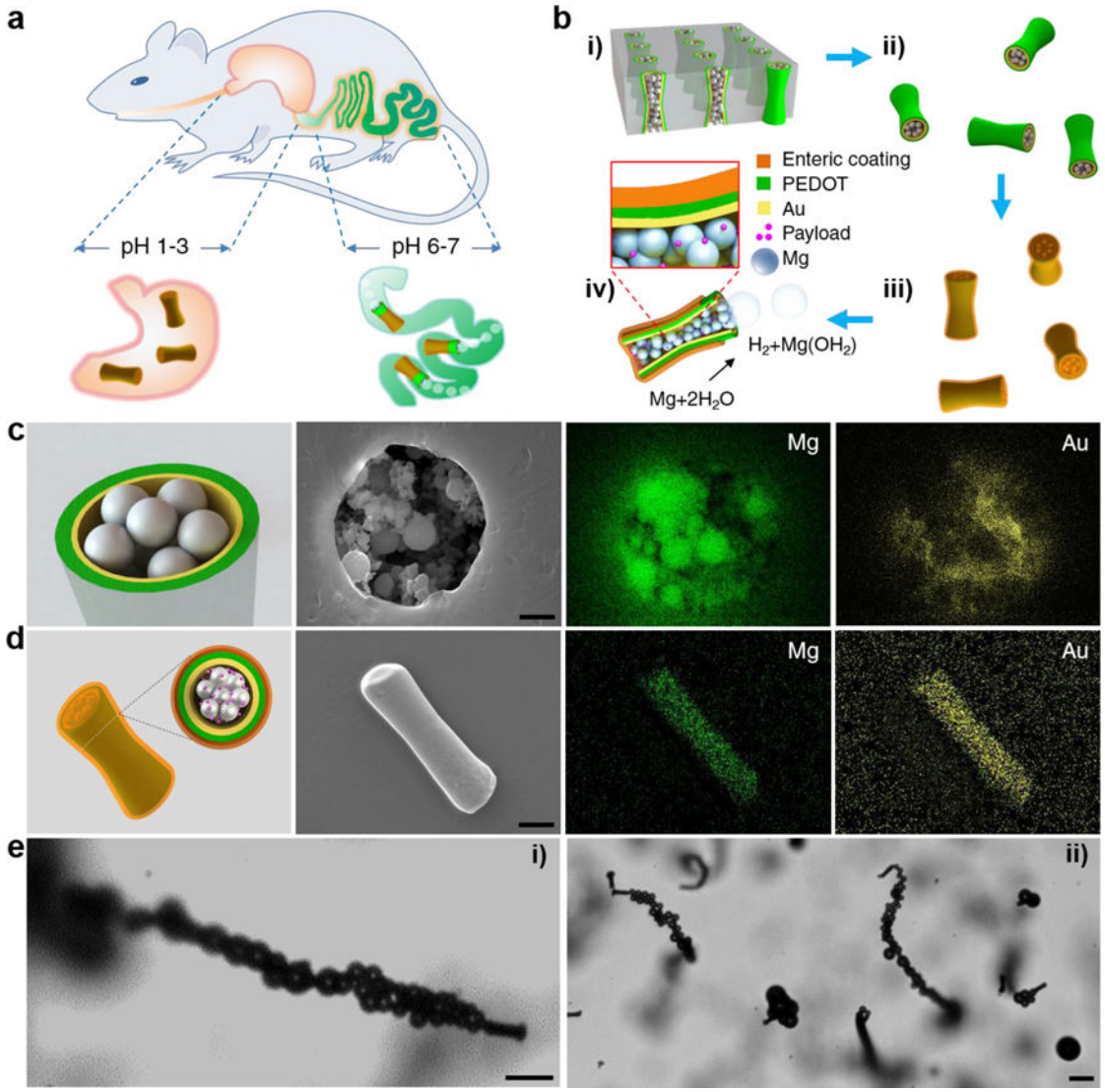

Figure 1. Synthesis and characterization of enteric magnesium micromotors (EMgMs)

(a) Schematic illustration of *in vivo* operation of the EMgMs for propulsion and localized delivery to the GI tract. (b) Preparation of EMgMs: (i) loading of Mg microspheres and payload into PEDOT/Au microtubes electrodeposited in microporous polycarbonate (PC) membrane with pore size of 5 μm and pore length of 15 μm; (ii) dissolution of PC membrane and release the Mg micromotors; (iii) coating Mg micromotors with enteric polymer; (iv) dissolution of the enteric coating and propulsion of Mg micromotors in solution with neutral pH. (c) Top view of a Mg micromotor with SEM characterization and EDX images of the Mg and Au in the micromotor. Scale bar: 1 μm. (d) Side view of an EMgM with SEM characterization and EDX images of the Mg and Au in the micromotor. Scale bar: 5 μm. (e) Propulsion snapshot of a single (i) and multiple (ii) EMgMs in the intestinal fluid. Scale bars, 20 μm.

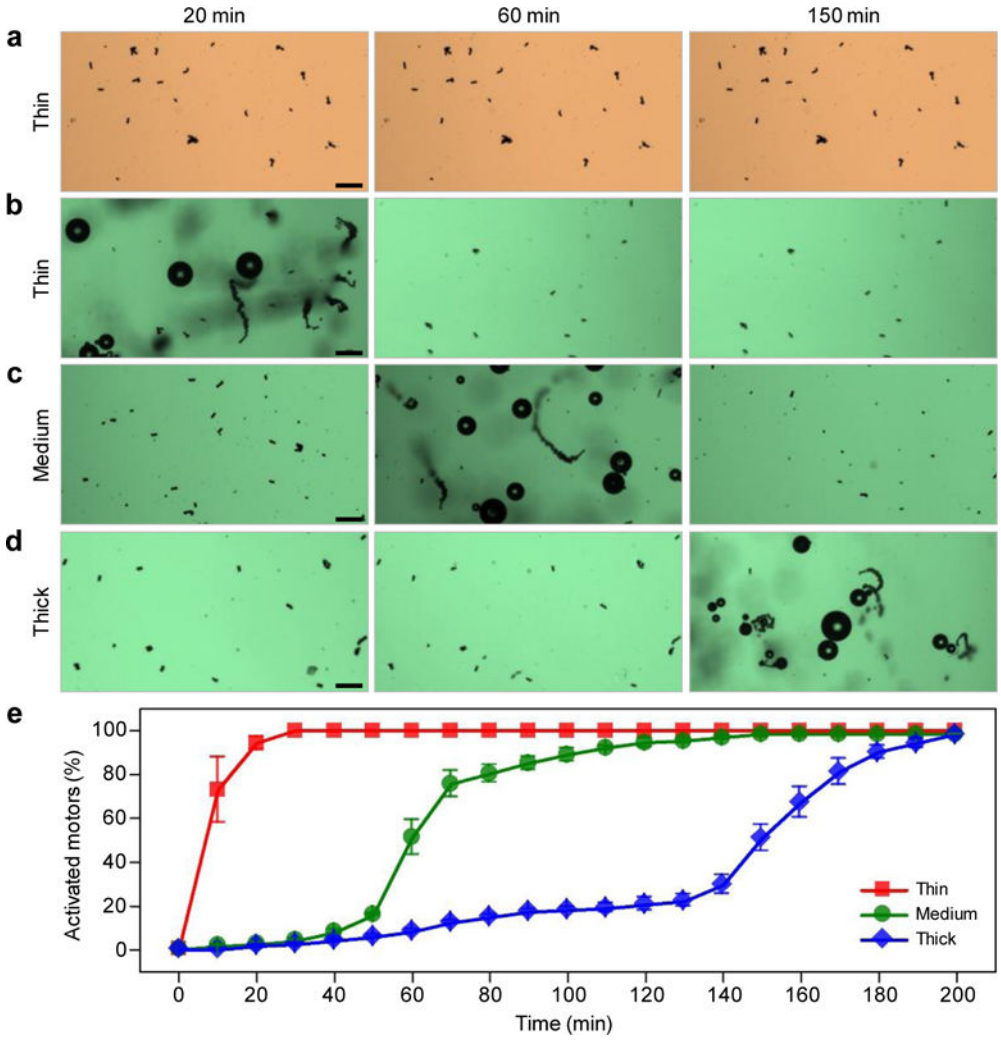

Figure 2. *In vitro* evaluation of EMgMs in gastric and intestinal fluids

(a) Microscopy images of EMgMs with thin thickness of enteric polymer coating immersed in gastric fluid for 20 min, 60 min and 150 min. (b–d) Microscopy images of EMgMs with thin (b), medium (c) and thick (d) enteric polymer coating immersed in intestinal fluid for 20 min, 60 min and 150 min. Scale bar, 50 μm. The three coating thicknesses are 0.3, 0.8 and 1.2 μm, respectively. (e) Quantitative analysis of the percentage of activated micromotors in intestinal fluid at different time points (n=6 with 400 micromotors in each test).

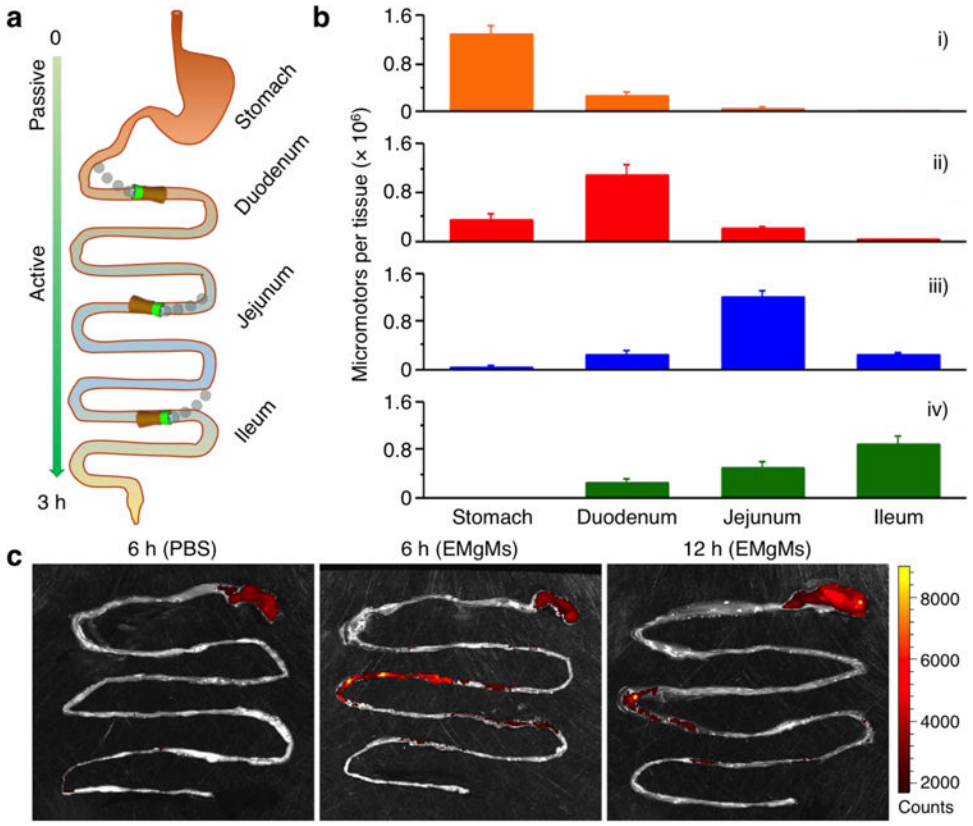

Figure 3. ***In vivo*** **biodistribution and retention of EMgMs in the GI tract**

(a) Schematic representation of the localization and retention of the micromotors in the stomach and GI tract. (b) ICP-MS analysis of the number of micromotors with different enteric coating thickness retained in the stomach, duodenum, jejunum, and ileum 6 hours post oral administration. The samples include (i) bare Mg micromotors without enteric coating, (ii) EMgMs with thin polymer coating, (iii) EMgMs with medium polymer coating, and (iv) EMgMs with thick polymer coating (n = 6 mice per group; estimation of number of the motors in each administration can be found in Supporting Note). (c) Superimposed fluorescent images of mouse GI tracts at 6 hours and 12 hours post-administration of EMgMs loaded with the dye Rhodamine 6G and covered with medium polymer coating. PBS was used as a control.

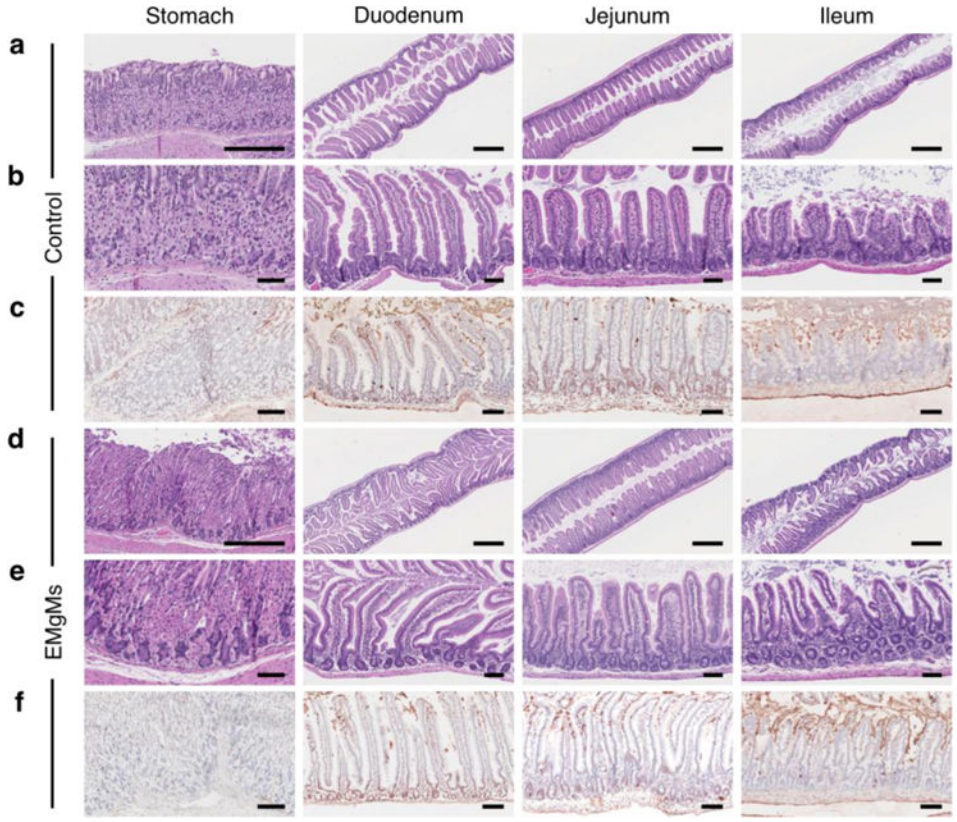

Figure 4. Toxicity evaluations of EMgMs

The stomach, duodenum, jejunum and ileum of mice treated with (a–c) PBS buffer or (d–f) EMgMs with medium polymer coating thickness were collected and analyzed. At 24 hours post-treatment, the mice were sacrificed and GI tract tissue sections were stained with H&E assay (a, b, d, and e) and TUNEL assay (c, and f). Scale bar (a, d: 500 μm; b, c, e, and f: 100 μm).